

Article

Safety Evaluation and Energy Consumption Analysis of Deep Foundation Pit Excavation through Numerical Simulation and In-Site Monitoring

Ji Chen ^{1,2}, Qi Xu ¹, Xinyu Luo ¹, Angran Tian ^{1,*}, Sujing Xu ³ and Qiang Tang ^{1,2,*}¹ School of Rail Transportation, Soochow University, Xiangcheng District, Suzhou 215131, China² Graduate School of Global Environmental Studies, Kyoto University, Sakyo-ku, Kyoto 606-8501, Japan³ Business School, Changshu Institute of Technology, Changshu, Suzhou 215500, China

* Correspondence: gangguo@126.com (A.T.); tangqiang@suda.edu.cn (Q.T.)

Abstract: Foundation pit excavation is common in urban construction, while safety evaluation is always significant in every specified project. The soil material properties, groundwater level, excavation method, supporting structure, monitoring points' arrangement, and so on distinguish from one site from another. Thus, many studies have looked into the safety and reliability of designated projects. This paper was based on the co-construction underground tunnel project of a deep foundation pit excavation in Suzhou, China. This paper aimed to perform a safety evaluation on this foundation pit by means of numerical simulation for parameter influence analysis, as well as scientific comparison with in-site monitoring data. To minimize the energy consumption and contribute to the carbon neutrality, a brief energy consumption analysis was also conducted. The results indicated that the maximum deformation of the foundation pit bottom is 4.5 cm and the deformation of the foundation pit is within the allowable range. The maximum horizontal displacement of each excavation is approximately at 10 m to 12 m of the diaphragm wall and the largest deformation is 28 mm. The maximum ground settlement is less than 16 mm, which confirmed the safety during excavation. It is ideal that the above deformation law will provide a reference for similar projects. Furthermore, this research simulated and monitored the whole cycle of foundation pit excavation, and contributes to savings in energy consumption and limiting of carbon emissions.

Keywords: foundation pit; energy consumption; deformation law; sensitivity analysis



Citation: Chen, J.; Xu, Q.; Luo, X.; Tian, A.; Xu, S.; Tang, Q. Safety Evaluation and Energy Consumption Analysis of Deep Foundation Pit Excavation through Numerical Simulation and In-Site Monitoring. *Energies* **2022**, *15*, 7099. <https://doi.org/10.3390/en15197099>

Academic Editor: Kyung Chun Kim

Received: 31 August 2022

Accepted: 22 September 2022

Published: 27 September 2022

Publisher's Note: MDPI stays neutral with regard to jurisdictional claims in published maps and institutional affiliations.



Copyright: © 2022 by the authors. Licensee MDPI, Basel, Switzerland. This article is an open access article distributed under the terms and conditions of the Creative Commons Attribution (CC BY) license (<https://creativecommons.org/licenses/by/4.0/>).

1. Introduction

As the city taps into the potential in deeper underground space, large-scale excavation in urban underground construction has become the norm. The excavation process is complex and many factors need to be considered, concerning the soil properties, supporting structure, the diaphragm wall, and even the materials utilized in the project [1,2]. The excavation deformation of large-scale foundation pit in this kind of stratum is large and difficult to control. With the increasing excavation of deep foundation pits, the design and construction of support structure are far more difficult than in conventional projects, resulting in an increased risk of implementation. This is because of the difficulty in effectively reducing structural deformation and soil disturbance, which puts forward higher requirements for safety evaluation and reliability conformation [3–5].

Many scholars have studied how to control the deformation in the process of deep foundation pit excavation by means of theoretical analysis, numerical calculation, and field monitoring. At present, most of the numerical calculation methods are used to simulate the excavation process of deep foundation pit and calculate and predict the deformation of retaining structure and soil. In the simulation process, each stage of foundation pit excavation can be considered to evaluate the disturbance of foundation pit excavation to its retaining structure deformation and surrounding buildings [6,7]. In order to summarize

more experiences from foundation pit excavation, the geometric parameters, soil properties, and diaphragm wall properties of foundation pits can be changed, and the influence law of stress and deformation of foundation pit construction structure can be analyzed. Numerical simulation may not be used for obtaining design parameters, but can be used as a reference for engineering construction.

The comparison with monitoring data and theoretical calculation results can provide a valuable reference for engineering practice [8–10]. Many studies have been based on the research of wall displacement and ground-surface settlement or support structure deformation through in-site monitoring or simply numerical simulation [11–13]. Some others focused on the effect of changes in groundwater level. The influence inside and outside the foundation pit was researched to determine the stability under specific rainy weather or water gushing during construction [14,15]. The monitoring technology was also studied and some newly developed monitoring machine with high precision has already been applied. Furthermore, with the carbon neutrality initiative proposed worldwide, scientific research gives more angles on environmental protection and energy saving, with the initial base of the safety guarantee of engineering. There is a case study that used metro line energy management center (MLEMC) in a vertical pit blasting project and studied the response characteristics of building structures during the blasting of subway foundation pit engineering [16]. It is innovative to combine the energy consumption theory and safety evaluation.

To contribute to energy saving and environmental protection, studies have been conducted on waste material utilization, environmental-friendly material usage, and even life cycle carbon calculation and energy consumption evaluation for a better arrangement in constructions [17,18]. Tang, et al. put much effort into the solid waste utilization in urban construction such as road pavement material [19–21]. Gu, et al. used recycled contaminated soil as the embankment in highway constructions [22,23]. Aside from the materials, the strategies and application of sustainable energy systems have also been investigated in recent years [24]. Thus, the energy evaluation and environmental analysis were combined in many studies [25,26].

This paper was based on a project in Suzhou, China. The silt layer there is deep, with remarkable characteristics of high compressibility, high water content, low bearing capacity, and strong flow plasticity. Thus, the excavation process in such a typical soil layer is worth researching. In this paper, we use the numerical simulation method to establish a foundation pit model, and use the model parameters to calculate and study the stratum deformation under different excavation steps. At the same time, the horizontal displacement of the diaphragm wall along the depth direction under different excavation steps is also studied in this paper. The surface settlement on both sides of the foundation pit is also analyzed. Finally, the influence of various parameters on the deformation of foundation pit and diaphragm wall is discussed. The energy consumption saving ratio is also estimated. In this paper, we intended to perform a thorough safety evaluation of a deep foundation pit with a typical soil layer background, in order to achieve the goal of energy saving and environmental protection and to be a reference for other similar foundation pit excavation projects.

2. Project Overview

The dimensions of this foundation pit and soil layer properties are presented here. Moreover, detailed information about the numerical model and monitoring points is shown in Section 2.1.

2.1. Structure Dimensions

The scene image of the foundation pit is shown in Figure 1a. The foundation pit was constructed in Suzhou, China. Concerning the material usage of the structure, the top of the foundation pit is supported by concrete and surrounded by concrete coupling beams. The internal support of the foundation pit is divided into three layers, all of which are

steel supports. The gap between the supports of each layer is 3.5 m. Meanwhile, two underground diaphragm walls with a depth of 20 m exist on both sides of the foundation pit. The overlapping structure of each layer of support in the foundation pit is a vertical lattice column.

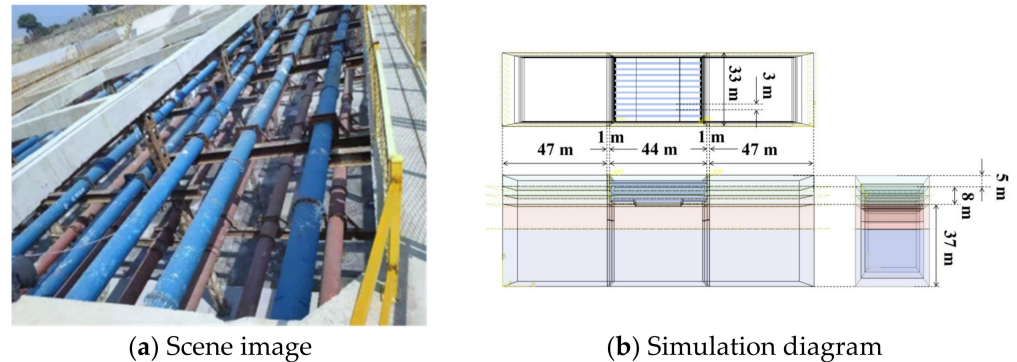


Figure 1. The structure of the foundation pit.

As shown in Figure 1b, the foundation pit model is 138 m long, 50 m high, and 33 m long in the direction of the foundation pit. Three layers of soil can be seen from the figure. At the same time, there are 11 steel supports with an interval of 3.3 m. The width of the diaphragm wall is 1 m, the slope angle of the pit bottom is simplified as vertical, and the depth of the bottom slope is about 1.5 m.

2.2. Parameters of Soils and Materials

The physical and mechanical parameters of the soil layer in the foundation pit are shown in Table 1. The soil layer is divided into seven layers, mainly clay. The parameters of the first three layers are similar, while the characteristics of the middle two layers are almost the same, and there is little difference between the bottom two layers.

Table 1. Physical and mechanical parameters of the soil layer in the foundation pit.

Soil Layer Name	Thickness of Soil Layer (m)	Density (g/cm ³)	Cohesion (kPa)	Friction Angle (°)
Miscellaneous fill	4.2	1.88	10	8
Silt	2.2	1.89	26.8	14.5
Silt mixed with silty clay	6.9	1.75	13.5	12.3
Clay	2.5	1.95	47.4	15.7
Silty clay	2.6	1.92	34.8	16.3
Sandy clay	5.7	1.86	7.6	24.1
Silt	7.3	1.87	2.8	14.3

Therefore, in this foundation pit simulation, these seven soil layers were simplified into three layers, as shown in Table 2.

Table 2. Physical and mechanical parameters of simplified soil layers.

Soil Layer Name	Thickness of Soil Layer (m)	Density (g/cm ³)	Cohesion (kPa)	Friction Angle (°)	Elastic Modulus (MPa)
Silty clay	5	19.2	34.8	16.3	25
Silty sand	8	18.7	2.8	28.9	50
Silty clay	37	19.6	45.4	16.2	30

The relevant parameters of other materials are shown in Table 3. In order to facilitate modeling and meshing, the support system is simplified in this paper. The internal support

is only three layers of steel support, and the vertical overlapped lattice columns are not presented in this simulation.

Table 3. Support structure parameters.

	Geometric Properties	Density (g/cm ³)	Elastic Modules (MPa)
Steel support	D = 800 mm, t = 20 mm	7.8	210,000
Diaphragm wall	D = 800 mm, spacing 1000 mm	2.4	30,000
Soil	(None)	<2	30
Reinforcement	(None)	>2	300

2.3. Monitoring Methods

In order to investigate the comparison of stress, deformation, and other related parameters between the structure and foundation pit in the process of excavation, this paper compares actual monitoring data and numerical simulation results. These monitor points are set inside the foundation pit, with only one exception, as shown in the Figure 2. The monitoring points were divided for the diaphragm wall, crown beam, column, and ground for the deformation and stress change through the whole excavation and construction process.

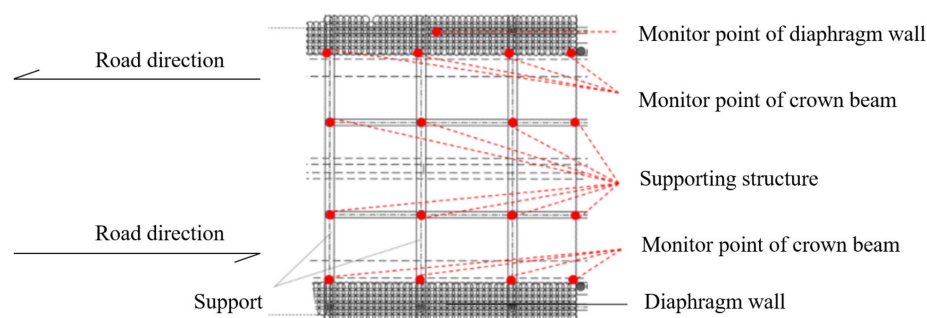


Figure 2. Layout of monitor points.

2.4. Mesh and Boundary Conditions

The meshing of the foundation pit model adopts a dense mesh in the small parts, which can make the calculation iteration more sufficient and reduce the possibility of calculation decoupling. As shown in Figure 3a, the mesh is dense at the slope in the bottom of the foundation pit, while it is sparse in the deep soil layer. The mesh here is distinguished from the top to the bottom, based on the intensity of the mesh and segments. The soil used was Moore Cullen Model, the concrete was the plastic damage model, and the steel supporting structure was the elastic model. Furthermore, there are two different boundary conditions in this model. The boundary condition on the side of the foundation pit is set to two degrees of freedom, which is assumed to be infinite along the direction of the foundation pit. The boundary conditions on both sides of the soil are completely fixed.

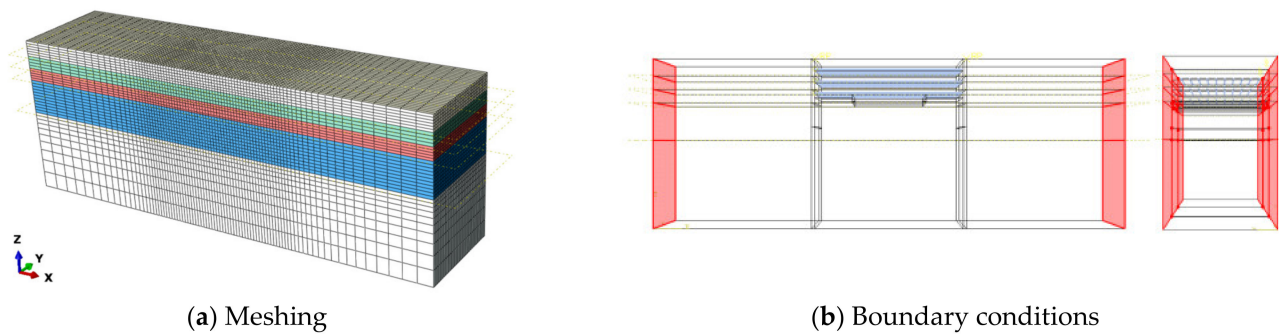


Figure 3. Meshing and boundary conditions' setting.

3. Monitored Data during Construction

In this section, the monitoring data will be shown from four parts, respectively. These data will be compared with simulation results in Section 4.

3.1. Groundwater Level

In the process of foundation pit excavation and support structure construction, the groundwater level was monitored. The monitoring process continued throughout the whole construction period, almost 200 days. For the most part, the groundwater is often between 0.5 m and 2.5 m underground. In order to facilitate construction and prevent foundation pit damage or water gushing, the depth of groundwater in the foundation pit needs to be dehydrated below 1 m underground. The foundation pit adopts a pipe well for dewatering, and the cement gravel filter pipe is wrapped with nylon mesh, with a longitudinal spacing of 10 m. The pipes are arranged horizontally along the foundation pit and the widened section is properly dense. Through drainage, the water level outside the pit is 13 m, and the water level remains constant during excavation to reduce the impact of the water level on construction [27,28].

The monitoring data of groundwater level during the project are shown in Figure 4. During the first 40 days of monitoring, there were error data, caused by the sudden rise in the water level caused by precipitation. Generally speaking, the groundwater level decreases with the increase in time. The groundwater level remained stable after 50 days of pumping. With the progress of pumping, the groundwater level will recover in a short time. Precipitation monitoring during foundation pit construction is helpful to control groundwater seepage and ensure the safety of foundation pit construction [29,30].

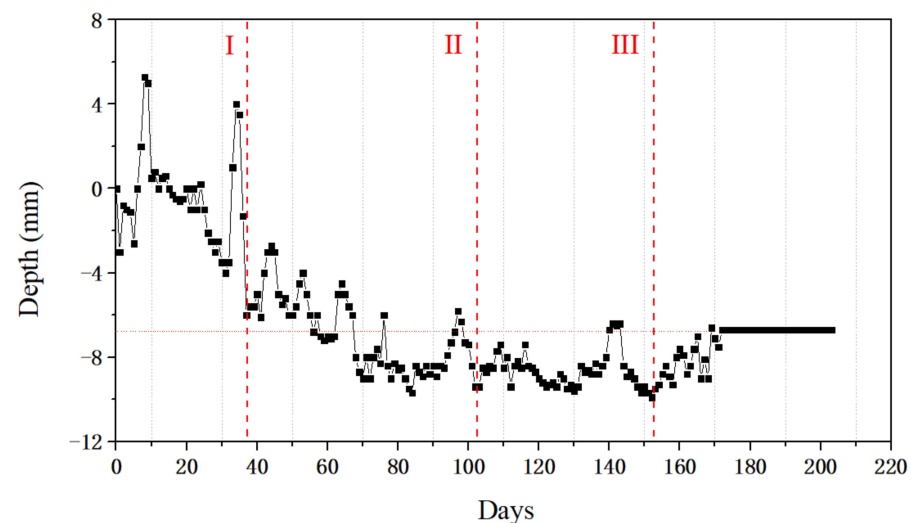


Figure 4. Groundwater level with time.

3.2. Displacement of Diaphragm Wall

The horizontal displacement of the diaphragm wall along the depth is the key to investigate the deformation of the diaphragm wall. A total of four monitoring points in the pit were set during the project, as shown in Figure 5. The monitoring data of two different measuring points are shown, where Figure 5a,b are the monitoring data of 25 m deep diaphragm wall and (d) are the monitoring data of 17 m diaphragm wall. It can be seen from the deep horizontal displacement diagram of underground diaphragm wall at four measuring points in the figure that the horizontal displacement curve of the underground diaphragm wall basically presents the phenomenon of “waist drum” with small ends and a large middle. With the increase in the excavation depth, the maximum horizontal displacement of the underground diaphragm wall gradually increases, but from the perspective of numerical value, the maximum horizontal displacement of underground diaphragm wall is within the specification control requirements [31].

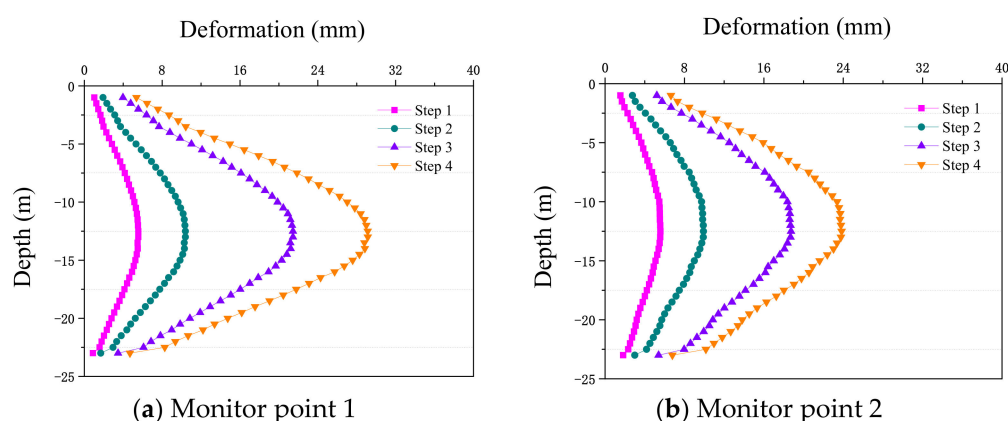


Figure 5. Horizontal displacement of the diaphragm wall through depth (monitored data).

The horizontal displacement curve of diaphragm wall can be roughly divided into four types, and the “bow” curve is mainly reflected in the deep soft stratum, and it is most common when the supported retaining wall is not buried deep under the pit bottom. The middle of the wall body arches out into the pit, and there is no obvious reverse bending point under the foundation pit [32,33].

The soil layer of the project has a typical binary sedimentation law, and the deformation form of the foundation pit retaining wall also has a certain law. According to the measured curve law of horizontal displacement of the diaphragm wall in deep foundation pits, the bow deformation curve in Figure 5 is closely related to the stratum distribution of the site and the form of foundation pit support. Firstly, the support form of the foundation pit is the support system of diaphragm wall and internal support. Secondly, the groundwater level of the foundation pit is high, and the site stratum has a typical binary sedimentation law. The upper stratum is a soft soil layer, and the lower stratum is relatively good, which is consistent with the occurrence factors described by the deformation form of the bow curve [34,35].

The position of the maximum horizontal displacement of the retaining structure of the foundation pit is not invariable; it will change with the excavation depth. At the initial stage, because of the unformed internal support, the deformation of the retaining wall is similar to that of the cantilever, and the maximum horizontal displacement occurs at the wall top. However, with the continuous increase in the excavation depth and the erection of the internal support, the horizontal displacement of the wall top is limited, and the position of the maximum horizontal displacement of the wall body gradually moves downward. The location of the maximum horizontal displacement is related to many factors [36,37].

From the first three points, the maximum horizontal displacement of the diaphragm wall occurred at about 12.5 m underground. The curve trend of the three measuring points in the four steps of foundation pit excavation is basically the same. It is worth

mentioning that the horizontal displacement of the wall after the first two excavation steps is within 10 mm, while the transverse deformation increases significantly in the third excavation and the fourth excavation. This may be because, after three excavations, the inner support structure reaches three layers, resulting in the redistribution of stress in the support structure. The bending moment in the middle of the wall increases, which causes the horizontal displacement of the wall to rise rapidly. The maximum horizontal displacement of the wall at the end of the excavation step is about 29 mm, while the displacement of the third measuring point is relatively small, only 24 mm. The wall of the fourth measuring point is 17 m and its horizontal displacement distribution is different. Generally speaking, the horizontal displacement of diaphragm wall is within the safe range and the excavation quality of foundation pit is pretty good [38,39].

The curve of horizontal displacement on the top of diaphragm wall during excavation is shown in Figure 6. As the wall of monitoring point 4 is 17 m, only the data of the first to third measuring points are compared, from the curve of horizontal displacement on the top of diaphragm wall. With the increase in the excavation depth, the horizontal displacement on the top of diaphragm wall first increases and then tends to be stable, which is basically unchanged in 60 to 70 days of excavation. From the numerical point of view, the maximum displacement is between 5 and 8 mm, thus the stability of the foundation pit is guaranteed [40].

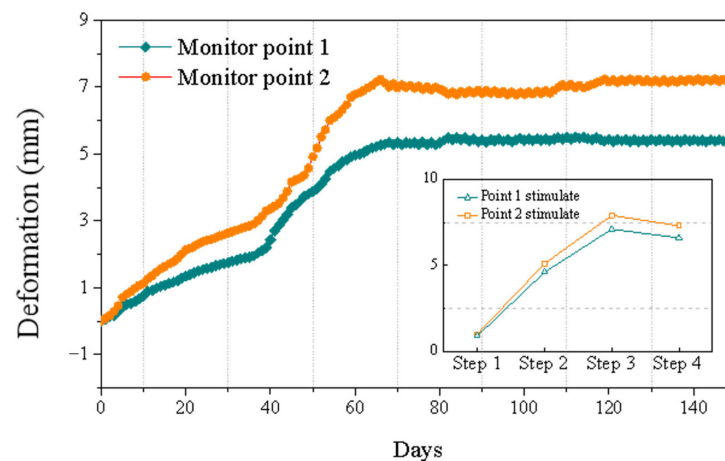


Figure 6. Horizontal displacement on top of the diaphragm wall.

3.3. Differential Settlement of Column

The foundation pit support structure is composed of an underground diaphragm wall and horizontal steel support, and the steel support is overlapped with the vertical lattice column. In this study, six columns were selected to monitor the differential settlement and the results are shown in Figure 7. The trend of the six monitoring points is basically the same, increasing first and then gradually becoming stable. The differential settlement of all columns reached equilibrium after three months. Among them, the first three measuring points showed an uplift trend in the first 20 days, which is mainly owing to the soil uplift caused by the unloading of the soil after the foundation pit excavation, the stress release at the bottom of the foundation pit, and the upward movement of the column. However, with the increase in the support structure and construction load, the upper load on the column increases, which gradually leads to settlement. In the next few months, the rise and settlement of the column are carried out alternately. Therefore, the reciprocating process of rising and falling needs to be controlled [41,42].

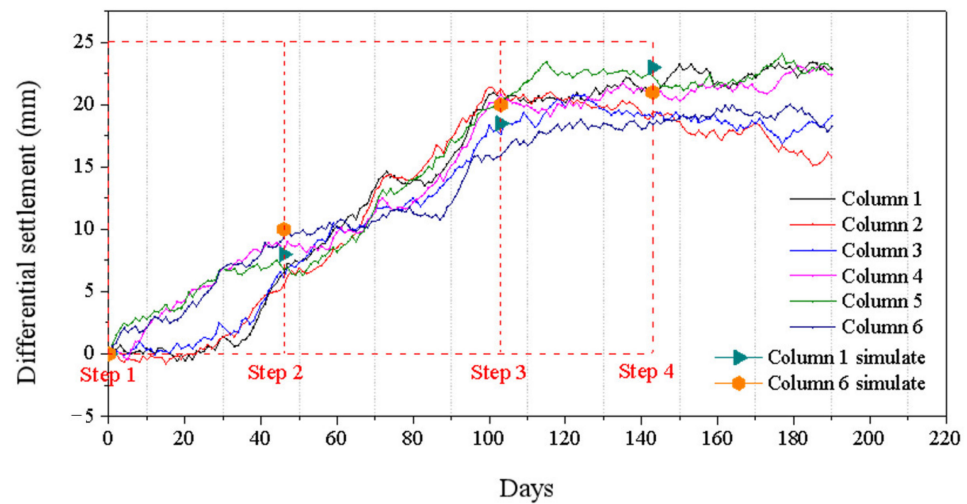


Figure 7. Differential settlement of the column during excavation.

The repeated up and down displacement of the column makes the soil loose, and the stress field of the stressed structure of the foundation pit is repeatedly balanced, resulting in uneven settlement in this process. Excessive uneven settlement will lead to column instability and affect the safety and stability of the support structure system. In general, in the process of foundation pit excavation, the uneven settlement of columns increases rapidly and remains relatively stable in the non-excavation period. During the whole excavation process, the maximum settlement of the column is about 24 mm, which is small and within the allowable range, and does not affect the stability of the support system or endanger the safety of the foundation pit [43,44].

3.4. Displacement of Crown Beam

A reinforced concrete crown beam is set at the top of the foundation pit and a reinforced concrete ring beam is set around the foundation pit. The crown beam connects the lower lattice column with the support system, so that the internal support structure of the foundation pit becomes a complete stress system, preventing the collapse of the top edge of the foundation pit or shaft and bearing the force of some steel support or reinforced concrete support. However, if the deformation of the top beam is too large, it is very easy to cause the inclination of the lower column or the deformation of the pile. Therefore, the displacement monitoring of the reinforced concrete crown beam is particularly important, which is one of the important factors to ensure the safety of the foundation pit [45,46].

A total of eight measuring points at different positions are set up to monitor the displacement changes in the horizontal and vertical directions. As shown in Figure 8, the horizontal displacement and vertical displacement of the beam change during excavation. The variation trend of horizontal displacement and vertical displacement is basically the same, but the values are different. With the increase in time, the horizontal displacement and vertical displacement of foundation pit increase, which is consistent with the trend of uneven settlement of the column with time. When the excavation reaches a certain depth, the displacement of the top beam tends to be stable. After the excavation, the overall displacement of the beam is basically unchanged. During excavation, the maximum horizontal displacement of the top beam is close to 18 mm and the maximum vertical displacement is close to 15 mm. The displacement in both directions is relatively small, which can be ignored for foundation pit excavation, and will not affect the safety and stability during and after foundation pit excavation [47,48].

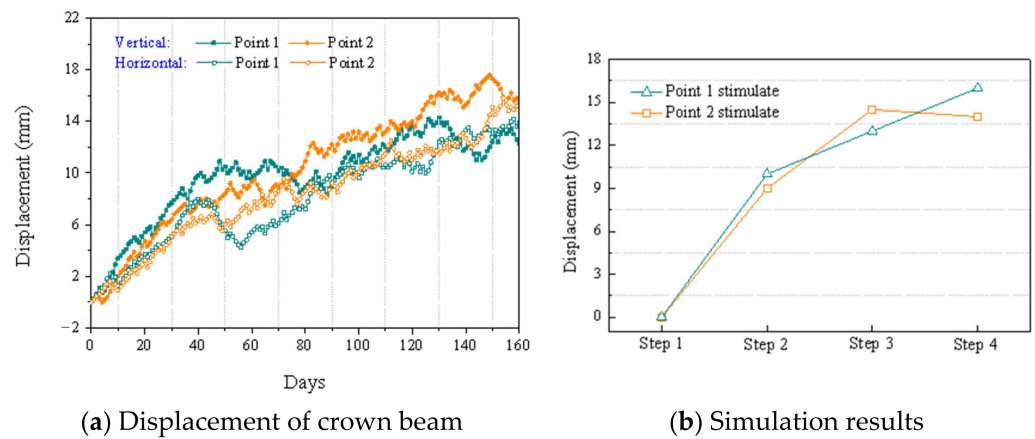


Figure 8. Horizontal and vertical displacement of the crown beam.

4. Results and Discussion

To analyze the safety and reliability of the excavation steps' arrangement and support structure stiffness, the monitoring data and simulation results were compared.

4.1. Vertical Displacement

The foundation pit excavation is divided into four steps. The first excavation is 3.5 m; the first support is set at 0.5 m above the pit bottom, while the second and third excavation along with the support are based on the first step. The fourth excavation step is at the middle slope in the deep bottom.

The vertical displacement of soil after model calculation is shown in Figure 9. After the first excavation, the maximum deformation of the foundation pit is 8.6 mm, the bottom of the foundation pit is uplifted, and the soil on both sides of the ground is slightly settled. After the second excavation, the uplift deformation of the pit bottom reached 2 cm. With only two excavations, the deformation is more than twice that of the first excavation. After the third excavation, the growth rate of pit bottom deformation is small, which is similar to that of the fourth excavation. Generally speaking, after the distributed excavation of the foundation pit, the deformation of the foundation pit is within the allowable range, far from reaching the failure form. The steep increase in the second excavation deformation may be caused by the small deformation of the first excavation, resulting in the redistribution of internal stress after the unloading of the second excavation soil [49,50].

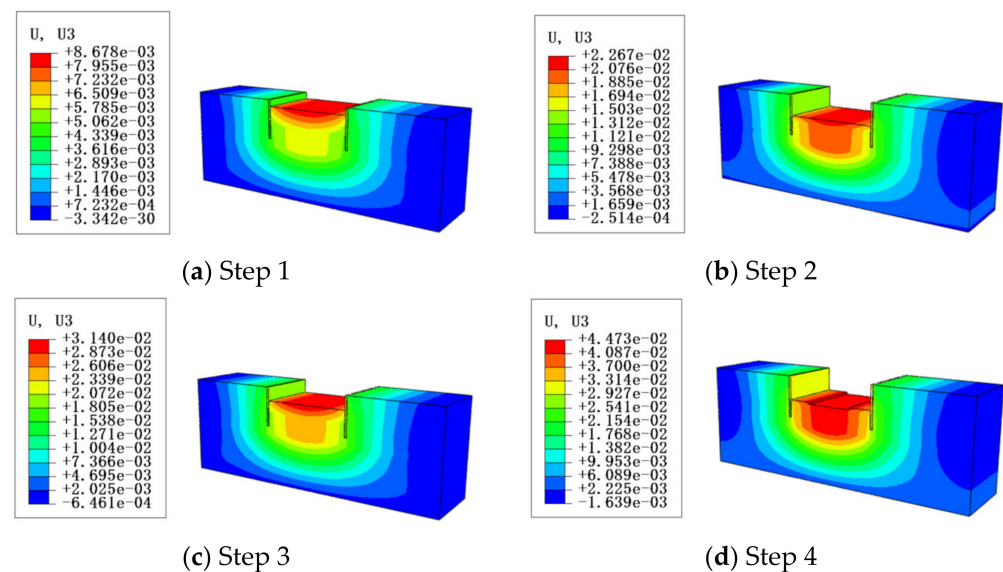


Figure 9. Vertical settlement.

4.2. Displacement in the Diaphragm Wall

During the whole excavation process, the deformation of the diaphragm wall is relatively small. As shown in Figure 10, the transverse deformation law of the diaphragm wall is basically the same. With the increase in the foundation pit excavation depth, it increases and then decreases. With the increase in the excavation depth, the lateral deformation of soil increases gradually. The maximum displacement of each excavation was witnessed at approximately 10 m to 12 m of the wall. In the fourth step of the excavation, the wall deformation was the largest, reaching 28 mm.

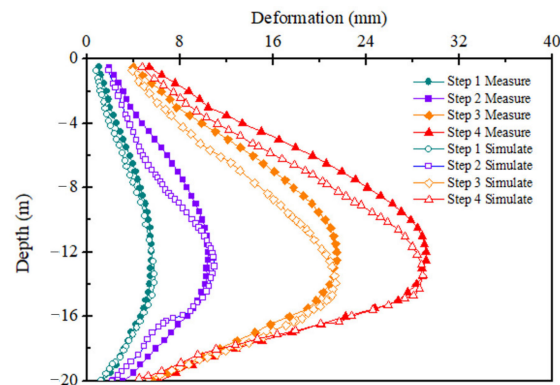


Figure 10. Horizontal displacement of the diaphragm wall through depth.

In general, the simulated value of the foundation pit is close to the actual monitoring value, and the predicted upper displacement is smaller than the actual monitoring value. The measured displacement of the lower part of the wall is relatively small, which may be caused by the failure to consider friction and other interactions between the wall and soil. After the third and fourth excavation, the wall deformation increases obviously, because the soil is unloaded and the walls on both sides are subjected to bending stress, which greatly increases the internal bending moment of the wall [26].

4.3. Ground Settlement

The variation trend of ground settlement in the foundation pit under different excavation steps is the same, as shown in Figure 11. Many studies have pointed out that the ground settlement will decrease first and then increase with the increases in distance, while the change trend of this simulation is single. This may be explained by the incomplete stress diffusion caused by the insufficient size of the model. In addition, the boundary conditions and the setting of the interaction between the wall and the soil layers also deserve further analysis. In this paper, the maximum ground settlement is less than 16 mm and the first excavation settlement is about 6 mm. Generally, such a small displacement means that the foundation pit excavation has little impact on the surroundings [51,52].

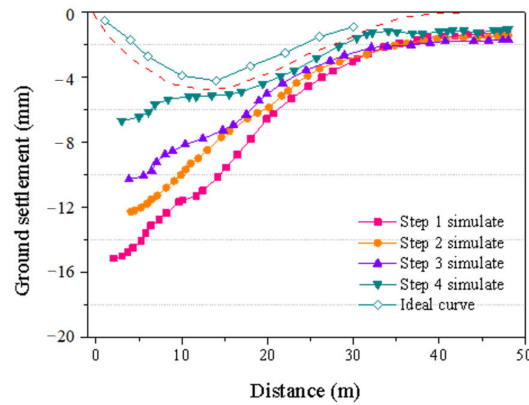


Figure 11. Ground settlement through excavation.

4.4. Influence of Parameters and Energy Consumption Analysis

In this section, cohesion, friction angle, elastic modulus, and insertion ratio are the four parameters analyzed, and the results are shown in Figure 12. The increase in cohesion causes the deformation to decrease slightly, and the change in the internal friction angle has little effect on the structural deformation. When the elastic modulus changes, the ground settlement decreases obviously, while the deformation of the diaphragm wall decreases slightly. The insertion ratio of the diaphragm wall has little effect on the ground settlement, and the deformation of the diaphragm wall decreases slightly with the increase in the insertion ratio. In general, the sensitivity of different parameters to the deformation of the diaphragm wall and the impact of the surrounding environment is relatively low, which represents that the relevant parameters of this simulation have certain applicability [53,54].

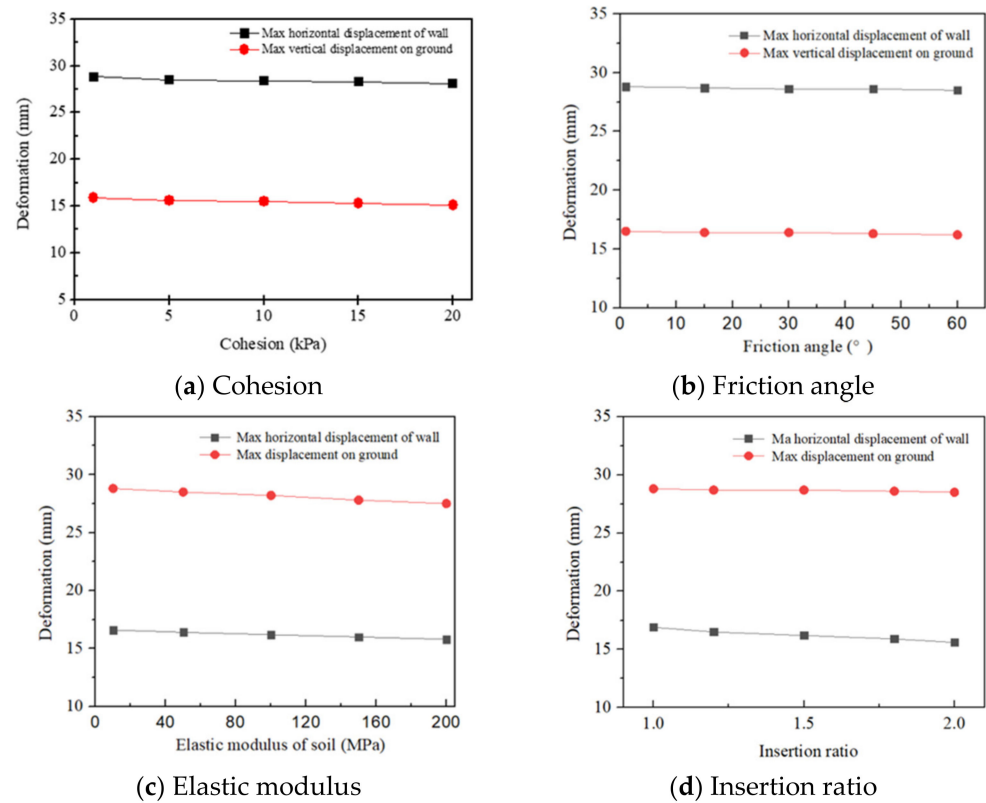


Figure 12. Displacement variation under different parameters.

The greenhouse gas emission in China was 140.93 billion tons in 2019, ranking top in the world, occupying 27% of the world’s total. At present, the annual consumption

of energy and carbon emission is still increasing. In the field of civil engineering, the main usages of energy are electricity and steam production and supply, while indirect energy consumption routings include the manufacture, production, and transportation of cement and cement asbestos products [55,56]. From the 1990s to the first 20 years of the 21st century, the carbon emission from civil engineering grew immensely, and a decrease was only witnessed in the recent few years. One reason may be the influence of COVID-19, but the main effect was the utilization of eco-friendly materials, like recycled aggregate from construction and demolition waste (CDW) or the advanced simulation and analysis mythologies before, during, and after the whole construction process. Our research was a case in the excavation of the foundation pit, potentially saving 10% in energy consumption, thus limiting carbon emissions to a great extent.

5. Conclusions

This paper investigates the deformation of a deep foundation pit based on numerical simulation. The influence of different parameters was also discussed and the energy saving ratio was estimated. The conclusions are as follows:

1. The maximum deformation of the foundation pit bottom is 4.5 cm. The deformation of the foundation pit is within the allowable range, far from reaching the failure form. The uplift of the foundation pit bottom is steadily increased.
2. The maximum horizontal displacement of each excavation is witnessed at approximately 10 m to 12 m of the diaphragm wall, and the largest deformation is 28 mm. The simulated value of the foundation pit is close to the actual monitoring value, but the friction and other interactions between the wall and soil need further study.
3. The variation trend of ground settlement in the foundation pit under different excavation steps decreases along the direction away from the foundation pit. The maximum ground settlement is less than 16 mm. The value change of four parameters has little effect on the simulation results of the foundation pit, which proves that the relevant parameters of this simulation have certain applicability.
4. This research simulated and monitored the whole cycle of foundation pit excavation, and contributes to the savings in energy consumption and limiting of carbon emissions.

Author Contributions: Conceptualization and methodology: Q.T.; formal analysis, software, and writing—original draft preparation: J.C. and Q.T.; validation: Q.X., X.L., and S.X.; writing—review and editing, A.T. All authors have read and agreed to the published version of the manuscript.

Funding: The research presented here is supported by the National Natural Science Foundation of China (52078317), Natural Science Foundation of Jiangsu Province for Excellent Young Scholars (BK20211597), project from Bureau of Housing and Urban-Rural Development of Suzhou (2021-25; 2021ZD02; 2021ZD30), Bureau of Geology and Mineral Exploration of Jiangsu (2021KY06), China Tiesiju Civil Engineering Group (2021-19), CCCC First Highway Engineering Group Company Limited (KJYF-2021-B-19) and CCCC Tunnel Engineering Company Limited (8gs-2021-04).

Institutional Review Board Statement: Not applicable.

Informed Consent Statement: Not applicable.

Data Availability Statement: The data presented in this study are available upon request from the corresponding authors.

Acknowledgments: Thanks to all authors' efforts and contributions.

Conflicts of Interest: The authors declare no conflict of interest.

References

1. Cui, K.; Feng, J.; Zhu, C.Y. A study on the mechanisms of interaction between deep foundation pits and the pile foundations of adjacent skewed arches as well as methods for deformation control. *Complexity* **2018**, *1*, 6535123. [[CrossRef](#)]
2. Ding, Z.; Jin, J.; Han, T. Analysis of the zoning excavation monitoring data of a narrow and deep foundation pit in a soft soil area. *J. Geophys. Eng.* **2018**, *15*, 1231–1241. [[CrossRef](#)]

3. Editorial Department of China Journal of Highway and Transport. Review on China's Subgrade Engineering Research. *China J. Highw. Transp.* **2021**, *34*, 1–49.
4. Zhang, J.; Li, J.; Yao, Y.; Zheng, J.; Gu, F. Geometric Anisotropy Modeling and Shear Behavior Evaluation of Graded Crushed Rocks. *Constr. Build. Mater.* **2018**, *183*, 346–355. [[CrossRef](#)]
5. Hou, S.; Chen, C.; Zhang, J.; Shen, H.; Gu, F. Thermal and mechanical evaluations of asphalt emulsions and mixtures for micro surfacing. *Constr. Build. Mater.* **2018**, *191*, 1221–1229. [[CrossRef](#)]
6. Fredlund, D.G.; Krahn, J. Comparison of slope stability methods of analysis. *Can. Geotech. J.* **1997**, *14*, 429–439. [[CrossRef](#)]
7. Gao, Y.; Zhang, Y.; Yang, Y.; Zhang, J.; Gu, F. Molecular dynamics investigation of interfacial adhesion between oxidized bitumen and mineral surfaces. *Appl. Surf. Sci.* **2019**, *479*, 449–462. [[CrossRef](#)]
8. Huang, M.; Liu, X.R.; Zhang, N.Y.; Shen, Q.W. Calculation of foundation pit deformation caused by deep excavation considering influence of loading and unloading. *J. Cent. South Univ.* **2017**, *24*, 2164–2171. [[CrossRef](#)]
9. Tang, Q.; Chu, J.M.; Wang, Y.; Zhou, T.; Liu, Y. Characteristics and factors influencing Pb(II) desorption from a Chinese clay by citric acid. *Sep. Sci. Technol.* **2016**, *51*, 2734–2743. [[CrossRef](#)]
10. Chen, R.P.; Meng, F.Y.; Li, Z.C.; Ye, Y.H.; Ye, J.N. Investigation of response of metro tunnels due to adjacent large excavation and protective measures in soft soils. *Tunn. Undergr. Sp. Technol.* **2016**, *58*, 224–235. [[CrossRef](#)]
11. Kammoun, Z.; Fourati, M.; Smaoui, H. Direct limit analysis-based topology optimization of foundations. *Soils Found.* **2019**, *59*, 1063–1072. [[CrossRef](#)]
12. Chen, S.; Cui, J.; Liang, F. Centrifuge Model Investigation of Interaction between Successively Constructed Foundation Pits. *Appl. Sci.* **2022**, *12*, 7975. [[CrossRef](#)]
13. Tang, Q.; Gu, F.; Gao, Y.F.; Inui, T.; Katsumi, T. Desorption Characteristics of Cr(III), Mn(II) and Ni(II) in Contaminated Soil Using Citric Acid and Citric Acid Containing Wastewater. *Soils Found (JGS)* **2018**, *58*, 50–64.
14. Han, S.Y.; Yang, K.; Wei, X.; Yun, L.; Cheng, C. Analysis of the influence of inside and outside water level changes of foundation pit on stability of foundation. *AER-Adv. Eng. Res.* **2016**, *99*, 280–284.
15. Xiong, B.L.; Wang, X.L.; Lu, C.J. High slope of prestressed anchor cable lattice beam reinforcement system 3D finite element analysis. *Railw. Constr.* **2010**, *2*, 67–70. (In Chinese)
16. Jiang, N.; Zhang, Y.; Zhou, C.; Wu, T.; Zhu, B. Influence of Blasting Vibration of MLEMC Shaft Foundation Pit on Adjacent High-Rise Frame Structure: A Case Study. *Energies* **2020**, *13*, 5140. [[CrossRef](#)]
17. Tang, Q.; Kim, H.J.; Endo, K.; Katsumi, T.; Inui, T. Size effect on lysimeter test evaluating the properties of construction and demolition waste leachate. *Soils Found (JGS)* **2015**, *55*, 720–736.
18. Zhang, Y.; Tang, Q.; Chen, S.; Gu, F.; Li, Z.Z. Heavy metal adsorption of a novel membrane material derived from senescent leaves: Kinetics, equilibrium and thermodynamic studies. *Membr. Water Treat.* **2018**, *9*, 95–104.
19. Tang, Q.; Zhang, Y.; Gao, Y.F.; Gu, F. Use of Cement-Chelated Solidified MSWI Fly Ash for Pavement Material: Mechanical and Environmental Evaluations. *Can. Geotech. J.* **2017**, *54*, 1553–1566. [[CrossRef](#)]
20. Zhou, Y.; Pan, L.; Tang, Q.; Zhang, Y.; Yang, N.; Lu, C. Evaluation of carbonation effects on cement solidified contaminated soil used in road subgrade. *Adv. Mater. Sci. Eng.* **2018**, *2018*, 5271324. [[CrossRef](#)]
21. Tang, Q.; Gu, F.; Chen, H.; Lu, C.; Zhang, Y. Mechanical Evaluation of Bottom Ash from Municipal Solid Waste Incineration Used in Road base. *Adv. Civ. Eng.* **2018**, 5694908. [[CrossRef](#)]
22. Zhang, J.; Gu, F.; Zhang, Y. Use of building-related construction and demolition wastes in highway embankment: Laboratory and field evaluations. *J. Clean. Prod.* **2019**, *230*, 1051–1060. [[CrossRef](#)]
23. Gu, F.; Zhang, Y.; Tang, Q.; Lu, C.; Zhou, T. Remediation of Zn(II) and Cu(II) contaminated soil using citric acid and citric acid containing wastewater. *Int. J. Civ. Eng.* **2018**, *16*, 1607–1619. [[CrossRef](#)]
24. Chu, W.; Calise, F.; Duić, N.; Østergaard, P.A.; Vicidomini, M.; Wang, Q. Recent Advances in Technology, Strategy and Application of Sustainable Energy Systems. *Energies* **2020**, *13*, 5229. [[CrossRef](#)]
25. Van der Male, P.; Vergassola, M.; van Dalen, K.N. Decoupled Modelling Approaches for Environmental Interactions with Monopile-Based Offshore Wind Support Structures. *Energies* **2020**, *13*, 5195. [[CrossRef](#)]
26. Hu, Y.; Yang, J.; Baniotopoulos, C. Study of the Bearing Capacity of Stiffened Tall Offshore Wind Turbine Towers during the Erection Phase. *Energies* **2020**, *13*, 5102. [[CrossRef](#)]
27. Li, J.W.; Li, X.; Xiong, M.X.; Luo, H.F. Deformation monitoring and numerical simulation of retaining structure in subway station deep foundation pit. *Electron. J. Geotech. Eng.* **2016**, *21*, 2331–2340.
28. Li, S.C.; Xie, C.; Liang, Y.H.; Qin, Y. Seepage flow model and deformation properties of coastal deep foundation pit under tidal influence. *Math. Probl. Eng.* **2018**, *2018*, 9714901. [[CrossRef](#)]
29. Mangushev, R.A.; Osokin, A.I.; Garnyk, L.V. Experience in preserving adjacent buildings during excavation of large foundation pits under conditions of dense development. *Soil Mech. Found. Eng.* **2016**, *53*, 291–297. [[CrossRef](#)]
30. Zhou, Y.; Su, W.J.; Ding, L.; Luo, H.; Love, P. Predicting safety risks in deep foundation pits in subway infrastructure projects: Support vector machine approach. *J. Comput. Civ. Eng.* **2017**, *31*, 04017052. [[CrossRef](#)]
31. Zhu, C.; Zhang, K.; Tao, Z.G.; An, B.; He, M.; Xia, X.; Liu, J. Combined application of optical fibers and CRLD bolts to monitor deformation of a pit-in-pit foundation. *Adv. Civ. Eng.* **2019**, *2019*, 2572034.
32. Zhu, C.; Yan, Z.H.; Lin, Y.; Xiong, F.; Tao, Z.G. Design and application of a monitoring system for a deep railway foundation pit project. *IEEE Access* **2019**, *7*, 107591–107601. [[CrossRef](#)]

33. Ou, M.X.; Liu, X.R.; Shi, J.X. Earth pressure applied in retaining wall of deep foundation pit considering influence of unloading and deformation. *Zhongnan Daxue Xuebao (Ziran Kexue Ban)/J. Cent. South Univ. (Sci. Technol.)* **2012**, *43*, 669–674.
34. Fan, S.; Song, Z.; Xu, T.; Wang, K.; Zhang, Y. Tunnel deformation and stress response under the bilateral foundation pit construction: A case study. *Arch. Civ. Mech. Eng.* **2021**, *21*, 1–19. [[CrossRef](#)]
35. Tang, Q.; Liu, W.; Li, Z.Z.; Wang, Y.; Tang, X.W. Removal of Aqueous Cu(II) with Natural Kaolin: Kinetics and Equilibrium Studies. *Environ. Eng. Manag. J.* **2018**, *17*, 467–476.
36. Kang, C.; Xu, R.; Ying, H.W.; Lin, C.; Gan, X. Simplified method for calculating ground lateral displacement induced by foundation pit excavation. *Eng. Comput.* **2020**. *ahead-of-print*.
37. Zheng, Y.; Hu, Z.; Ren, X.; Wang, R.; Zhang, E. The influence of partial pile cutting on the pile-anchor supporting system of deep foundation pit in loess area. *Arab. J. Geosci.* **2021**, *14*, 1–12. [[CrossRef](#)]
38. Wu, J.; Peng, L.; Li, J.; Zhou, X.; Sun, J. Rapid safety monitoring and analysis of foundation pit construction using unmanned aerial vehicle images. *Autom. Constr.* **2021**, *128*, 103706. [[CrossRef](#)]
39. Zhao, X.Y.; Zhang, Y.W.; Ding, H.; Chen, L.Q. Vibration suppression of a nonlinear fluid-conveying pipe under harmonic foundation displacement excitation via nonlinear energy sink. *Int. J. Appl. Mech.* **2018**, *10*, 1850096. [[CrossRef](#)]
40. Zhao, Z.; Lei, Y. Mechanism analysis of uncovering coal in crosscut and gas outburst based on flac3d. *J. Coast. Res.* **2020**, *103*, 333–338. [[CrossRef](#)]
41. Kim, K.Y.; Lee, D.S.; Cho, J.; Jeong, S.S.; Lee, S. The effect of arching pressure on a vertical circular shaft. *Tunn. Undergr. Space Technol.* **2013**, *37*, 10–21. [[CrossRef](#)]
42. Fang, Y.S.; Ishibashi, I. Static earth pressures with various wall movements. *J. Geotech. Eng.* **1986**, *112*, 317–333. [[CrossRef](#)]
43. Sarmadi, H.; Karamodin, A. A novel anomaly detection method based on adaptive Mahalanobis-squared distance and one-class kNN rule for structural health monitoring under environmental effects. *Mech. Syst. Signal Process.* **2020**, *140*, 106495. [[CrossRef](#)]
44. Liu, Z.P.; Liu, J.; Bian, K.; Ai, F. Three-dimensional limit equilibrium method based on a TIN sliding surface. *Eng. Geol.* **2019**, *262*, 105325. [[CrossRef](#)]
45. Wang, Y.K.; Sun, S.W.; Liu, L. Mechanism, Stability and Remediation of a Large Scale External Waste Dump in China. *Geotech. Geol. Eng.* **2019**, *37*, 5147–5166. [[CrossRef](#)]
46. Zheng, Y.; Chen, C.; Liu, T.; Zhang, H.; Sun, C. Theoretical and numerical study on the block-flexure toppling failure of rock slopes. *Eng. Geol.* **2019**, *263*, 105309. [[CrossRef](#)]
47. Cao, S.; Xia, L.X. Conscientiousness mediates the link between brain structure and consideration of future consequence. *Neuropsychologia* **2020**, *141*, 107435. [[CrossRef](#)]
48. Motta, E. Generalized Coulomb active-earth pressure for distanced surcharge. *J. Geotech. Eng.* **1994**, *120*, 1072–1079. [[CrossRef](#)]
49. Kshirsagar, N.A. Rational use of medicines: Cost consideration & way forward. *Indian J. Med. Res.* **2016**, *144*, 502.
50. Song, W.; Veenstra, J.A.; Perrimon, N. Control of lipid metabolism by tachykinin in *Drosophila*. *Cell Rep.* **2014**, *9*, 40–47. [[CrossRef](#)]
51. Finno, R.J.; Blackburn, J.T.; Roboski, J.F. Three-dimensional effects for supported excavations in clay. *J. Geotech. Geoenviron. Eng.* **2007**, *133*, 30–36. [[CrossRef](#)]
52. Gnanapragasam, N. Active earth pressure in cohesive soils with an inclined ground surface. *Can. Geotech. J.* **2000**, *37*, 171–177. [[CrossRef](#)]
53. Peters, G.P.; Weber, C.L.; Guan, D.; Hubacek, K. China's growing CO₂ emission—A race between increasing consumption and efficiency gains. *Environ. Sci. Technol.* **2007**, *41*, 17. [[CrossRef](#)] [[PubMed](#)]
54. Marinković, S.; Radonjanin, V.; Malešev, M.; Ignjatović, I. Comparative environmental assessment of natural and recycled aggregate concrete. *Waster Manag.* **2010**, *30*, 2255–2264. [[CrossRef](#)] [[PubMed](#)]
55. Fambri, G.; Badami, M.; Tsagkrasoulis, D.; Katsiki, V.; Giannakis, G.; Papanikolaou, A. Demand Flexibility Enabled by Virtual Energy Storage to Improve Renewable Energy Penetration. *Energies* **2020**, *13*, 5128. [[CrossRef](#)]
56. Kanz, O.; Reinders, A.; May, J.; Ding, K. Environmental Impacts of Integrated Photovoltaic Modules in Light Utility Electric Vehicles. *Energies* **2020**, *13*, 5120. [[CrossRef](#)]